JOURNAL OF MATERIALS SCIENCE 9 (1974) 911–919

The effects of pressurization on the microstructure and mechanical properties of magnesium oxide

M. S. STUCKE, A. S. WRONSKI
School of Materials Science, University of Bradford, Bradford, UK

Changes in microstructure in single crystals of MgO, containing elastic discontinuities, which result from pressurization treatments in the range 0.2 to 2 GN m^{-2} have been studied using an etch-pitting technique. Complex dislocation arrays have been observed around cubical and spherical cavities and precipitates. The observations are discussed in terms of stress and strain criteria. Production of {1 0 0} and {1 1 0} cracks at high pressure is also described. Following a 1 GN m^{-2} pressurization the flow stress was observed to decrease by < 10% and this has been related to the induced dislocation density. In polycrystalline MgO the fracture strength was unaltered by pressurization but the critical temperature difference of thermal shock, ΔT_C, was increased by 55 K. This has similarly been attributed to the movement of pressurization-induced dislocations.

1. Introduction

The irreversible effects of high hydrostatic pressures on the microstructure and mechanical properties of cubic [1, 2] and hexagonal [3] metals and alloys have lately received considerable attention and more recently similar studies have been performed on the cubic ionic solids NaCl [4-6] and LiF [7-9]. Although cubic solids are isotropic with respect to their linear compressibilities [10], when such a solid containing local elastic or plastic discontinuities, e.g. voids, precipitates or grain boundaries, is subjected to a high hydrostatic pressure, shear stresses can be generated in the matrix near these discontinuities. These stresses, if sufficiently high, are thought responsible for the production of dislocations [1, 11, 12]. In the studies of bcc metals these changes in microstructure have generally been inferred from the changes in mechanical properties observed after pressurization. For example, Bullen *et al* [13] and Mellor and Wronski [14] observed a lowering of the ductile-brittle transition temperature of Cr after "seasoning" treatments at pressures of the order of 1 GN m^{-2}.

The direct study of the generation of dislocations in some alkali halides [4-9] is greatly facilitated by using a dislocation etching technique. In this way the dislocation structure of the same volume of material before and after pressurization can be compared and any changes shown to be unequivocally due to the pressurization. This approach was also made in this work which is concerned with the pressurization-induced generation of dislocations around cavities and precipitates in monocrystalline MgO and the effect of pressurization on the mechanical properties of a commercial polycrystalline magnesia ceramic.

2. Experimental procedure

Single crystals of MgO containing Fe impurity were obtained from the Norton Co (Worcester, Mass, USA). On close examination certain areas of these crystals were found to contain cavities, many of which were roughly cubic in shape and varying in volume from approximately 10 to 200 μm^3. Other voids were spherical with diameters up to 20 μm. Some areas in the crystals were also found to contain precipitates, probably of metallic iron [15].

Crystals were prepared for microscopic examination by cleaving on {100} planes. Compression specimens were cut, also on {1 0 0} planes, using a diamond slitting saw; the damaged surfaces were removed by chemical polishing at 373 K in orthophosphoric acid. The samples' dimensions were approximately 3 mm × 3 mm × 7 mm and they were tested at room temperature on a Universal Hedeby machine at a strain-rate of 7×10^{-3} sec^{-1}. Dislocations were detected by etching the crystal surfaces with 1 part H_2SO_4, 1 part H_2O and 3 parts saturated solution NH_4Cl at room temperature.

The polycrystalline cold-pressed MgO was supplied as 12.5 mm diameter rods by Cerac Inc (USA). The average grain size was ~ 30 μm and the average density 96 to 98% of the theoretical value. The microstructure of this material was, however, too complex for etch pitting to be used as a method of studying dislocations. From the rods ring test specimens [16] were manufactured. These had an outside diameter of 12.5 mm, inside diameter of 4.1 mm and were 3 to 4 mm thick. The ring specimens were tested in compression between parallel hardened steel plattens attached to a motorized Hounsfield Tensometer. The loading rate was 2×10^{-4} mm sec^{-1} and the load was measured using a semiconductor load cell.

Specimens for thermal shock experiments were suspended individually on a thin wire, in air, in a vertical tube furnace. They were lowered slowly into the furnace, left to thermally stabilise for 30 min, then dropped into a beaker of water at room temperature and finally allowed to cool. The temperature drop, ΔT, was measured to $\pm$ 5K.

The pressurization of both single and polycrystalline MgO was carried out in a N.P.L.-type piston cylinder hydrostatic press at pressures up to 2 GN m^{-2} (20 000 atm.). The pressurizing fluid was iso-pentane. The polycrystalline specimens had to be placed in a thin rubber sheath to prevent penetration of the fluid into the pores of the material, since at high pressure penetration otherwise is considerable and severe cracking of the specimens had been detected in unsheathed samples.

3. Results

3.1. Generation of dislocations by pressurization in monocrystals

Following treatments at pressures in the range 0.2 to 2 GN m^{-2} dislocation arrays were detected around cavities by etching {100} planes (Figs. 1 to 4). The pressurization-induced dislocation loops which intersect these planes produce arrays in ⟨110⟩ and ⟨100⟩ directions, edge and screw arrays respectively. The appearance of the plastic zones closely resemble those found in LiF by previous workers [7-9]; sectioning by successive polishing and etching towards e.g. a 20 μm cubical cavity (Fig. 1) has shown dislocation loops to emanate from the twelve cavity edges on the {110} primary slip planes. Fig. 2 shows typical arrays generated by a spherical cavity of similar size, i.e. 20 μm in diameter, also pressurized at 2 GN m^{-2}. There are more active dislocation sources and the dislocation arrangement is obviously more complex than for the cubical cavity.

The threshold pressure for dislocation generation was cavity size dependent, e.g. a large void, approximately a 150 μm cube, produced arrays at a pressure of 0.2 GN m^{-2}, whereas a small cavity (20 μm cube length) remained inactive at pressures up to 1.0 GN m^{-2}. Similarly no dislocation activity was observed around spherical cavities 20 μm in diameter below 1.0 GN m^{-2}. The dislocation configuration produced by both cubical and spherical cavities became more complex with an increase in the "seasoning" pressure; the number of active sources increased and each wing became broader and longer. This is clearly shown in Fig. 3, which shows parts of several arrays generated by a large cubical cavity.

Since, on pressurizing, all six {110} slip

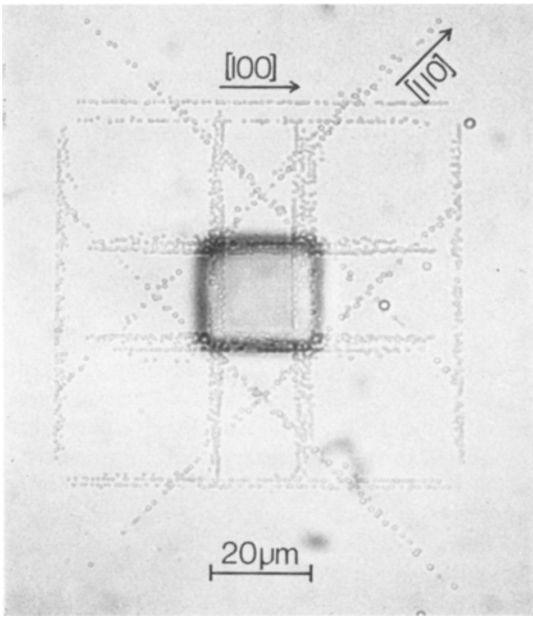

Figure 1 Typical etch pit arrays on a {100} plane in the vicinity of a 20 μm cubical cavity following pressurization of 2 GN m^{-2}. Dislocation arrays are observed on all six {110} slip planes containing or adjacent to a ⟨100⟩ cavity edge.

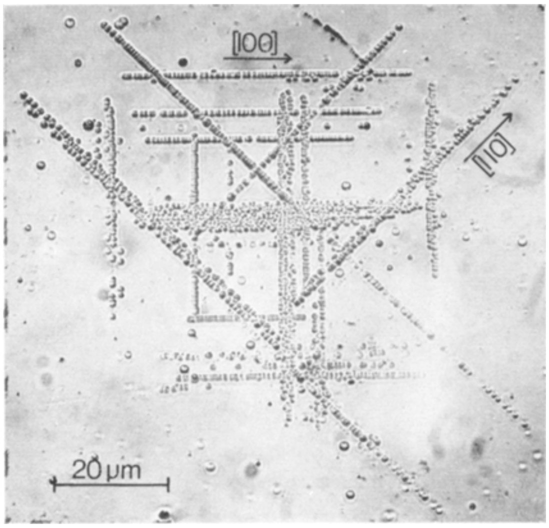

Figure 2 Typical etch pit arrays formed on a {100} plane near a spherical cavity, 10 μm radius, pressurized at 2 GN m^{-2}. The plastic zone is complex compared with cubical cavity in Fig. 1, but again arrays are observed on all six {110} glide planes.

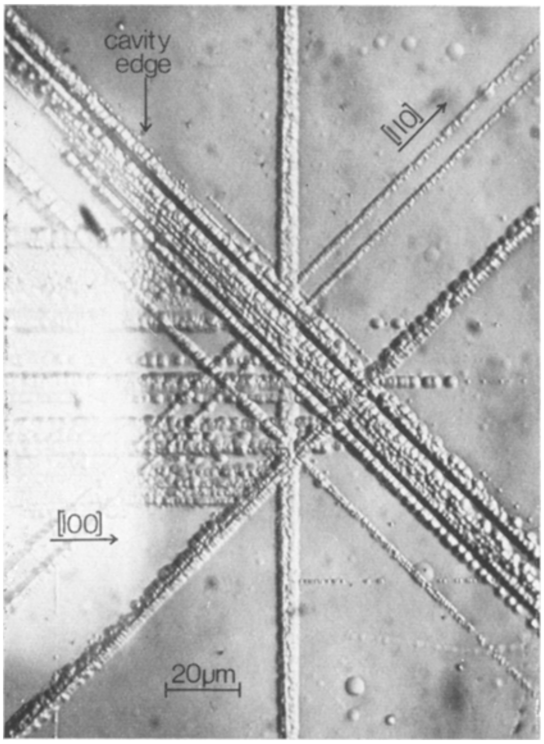

Figure 3 Part of a complex plastic zone, intersecting a {100} face, which was formed by a large cubical cavity in a crystal pressurized at 0.4 GN m^{-2}. The specimen was etched, repressurized at 0.5 GN m^{-2} and re-etched, thus the large etch pits are from dislocations produced at 0.4 GN m^{-2} and the smaller pits result from dislocations formed at the higher pressure. Note that most of the dislocations in the [100] arrays have not penetrated the oblique ⟨110⟩ slip bands. The presence of many "old" (flat-bottomed) etch pits in the [100] arrays indicates that the dislocations have moved into the oblique slip band during the higher pressurization.

planes are active in a small volume of material, both oblique and conjugate intersections of slip bands may occur. These bands can be broad and densely populated, especially following severe pressurizations. A closer examination of the [100] bands in Fig. 3 reveals flat-bottomed pits on the cavity side of the oblique ⟨110⟩ dislocation arrays, indicating that these dislocations (produced at a lower pressure, 0.4 GN m^{-2}), had moved away from the cavity, probably into the ⟨110⟩ slip bands. Only a few pits are present in the [100] arrays beyond the slip band showing that many dislocations have been unable to penetrate the oblique slip band. Dislocations intersecting conjugate slip bands, on the other hand, apparently have little difficulty in penetrating each other (Fig. 3).

Fig. 4 shows the effect of treatment at a relatively high pressure, 1.0 GN m^{-2}, on a large cavity. It is seen that {110} cracks have formed in addition to the extensive slip characteristic of the combination of high pressure and large cavity. {100} cracks were also formed, apparently emanating from the cavity faces.

Following pressurization at or above 1.5 GN m^{-2} dislocation arrays were also observed around the precipitates. Fig. 5 shows the microstructure produced at 2 GN m^{-2}. Again the similarity between these arrays and those from cubical cavities (Figs. 1 to 3) is striking.

The mobility of dislocations introduced by pressurization is illustrated by the ease with which they move under the influence of an applied uniaxial stress. Extensive movement of these dislocations at compressive stresses greater than half the yield stress have been observed at room temperature (Fig. 6). (These results contrast with those on pure LiF [8, 9].) Because of the scatter on the yield stress values of unpressurized specimens containing large numbers of precipitates, 80 to 110 MN m^{-2}, a direct comparison of the flow stresses of unpressurized and pressurized material was precluded. The

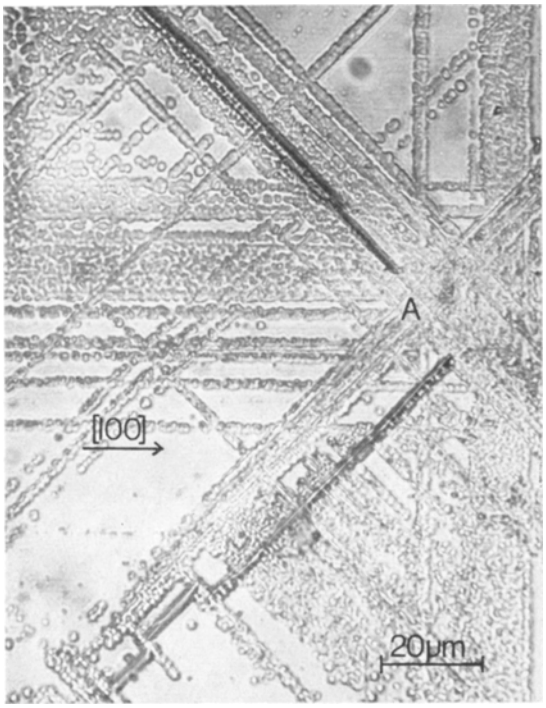

Figure 4 Typical cracks formed on {110} planes near a large cavity following pressurization at 1.5 GN m^{-2}. Note also extensive dislocation activity characteristically observed on all six {110} slip systems. The cracks are possibly initiated at the intersection of oblique and conjugate slip planes at A, where large anisotropic shear stresses will be present.

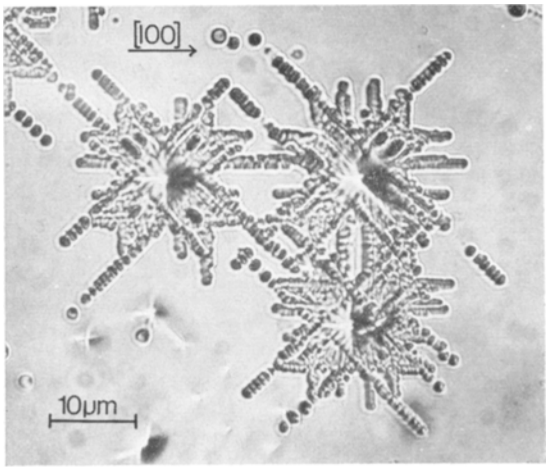

Figure 5 Intersection of a plastic zone, formed by precipitates pressurized to 2 GN m^{-2}, with a {100} face. Note the similarity between these arrays and those formed by cubical cavities (Fig. 1).

procedure adopted therefore was to load unpressurized samples in compression to above the yield stress, unload and pressurize at 2 GN m^{-2} and then reload. Decreases of up to 10% in the flow stress were observed. Reloading of unpressurized specimens resulted in changes in the recorded load to reinitiate plastic flow of $< 2\%$. No effects of pressurization on the work-hardening rate, in contrast to LiF [9], were detected.

3.2. Thermal shock and fracture strength of polycrystals

Specimens taken from three different rods of MgO were used for all the following tests. Random specimens were taken from the three batches of material and thermally shocked; the fracture strength data are shown in Fig. 7. No significant difference in behaviour between specimens from the different batches was detected. The strength of the unshocked material was found to be 150 $\pm$ 10 MN m^{-2}. This decreased sharply at the critical temperature difference of thermal shock, ΔT_C, to 45 $\pm$ 10 MN m^{-2}. The value of ΔT_C was found to be 155 $\pm$ 5K; ΔT_C was calculated at the mean stress level. No degradation of strength was observed below ΔT of 145K and no further decrease in strength was seen above ΔT of 165K (up to ΔT of 350K).

Specimens pressurized at 1.5 and 2 GN m^{-2} prior to thermal shock were found to have a higher $\Delta T_C \doteqdot 210 \pm 5$K (Fig. 7). The fracture strength of the unshocked but pressurized material remained at 150 $\pm$ 10 MN m^{-2}. The fracture stresses above and below ΔT_C appear not to be affected by the pressurization treatment.

The pressurization of specimens after thermal shocking produced no detectable effects on either ΔT_C or the two strength levels of the thermally shocked specimens.

4. Discussion

The similarity of the observed dislocation microstructure produced by pressurization around cavities and precipitates to those in conventionally deformed MgO [17] and those produced by indentation [18] leads us to doubt the hitherto generally held hypothesis (proposed as a result of experiments with cubic metals) that dislocation generation during pressurization is by prismatic punching [2], at least in MgO. Evans *et al* [8] have recently also shown that in

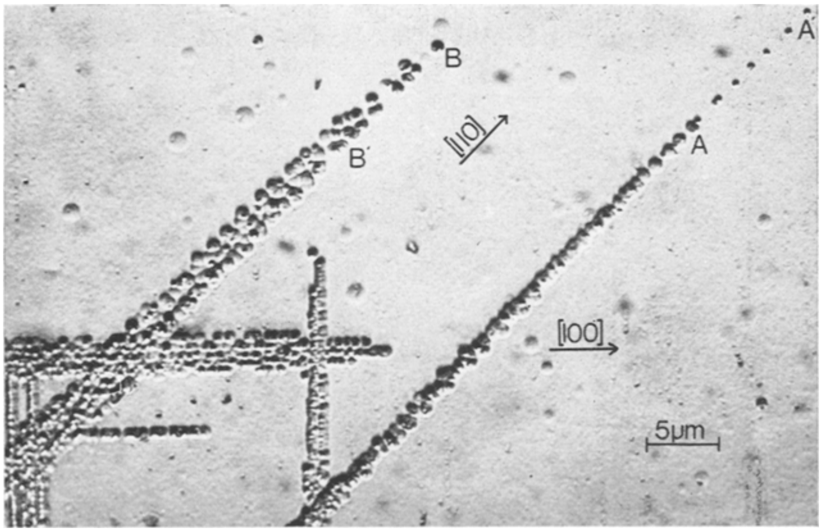

Figure 6 An illustration of the mobility of pressurization-induced dislocations. Note that dislocations have moved from A to A′ in one edge array after the crystal was compressed in the [010] direction to 0.6 of the flow stress. Concurrently dislocations in the parallel array have moved in the opposite direction, i.e. B to B′.

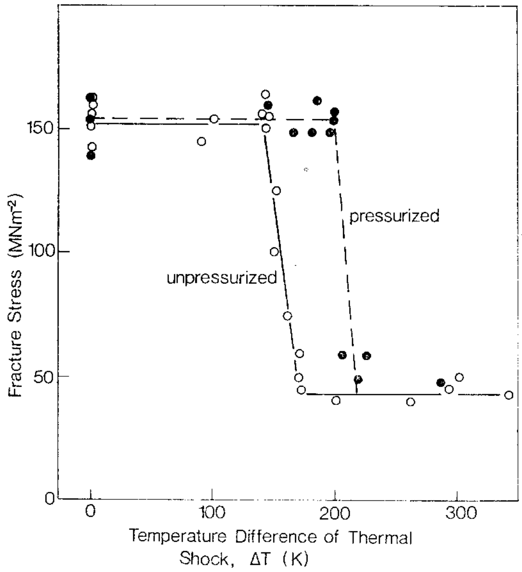

Figure 7 Strength at room temperature of MgO ring specimens which had been subjected to thermal shock. Open symbols refer to unpressurized specimens and the closed symbols refer to specimens pressurized at 2 GN m^{-2} prior to thermal shocking.

LiF containing cavities pressurization-induced dislocation generation is by a conventional slip process. Prismatic punching in a material possessing only two independent slip systems at the relevant temperature appears extremely unlikely, even more so if cross-slip is restricted, as it is in MgO [17]. Prismatic punching may well occur in materials containing five independent slip systems, such as AgCl and many metals. For MgO, however, any dislocation generation model, it is suggested, must involve conventional slip processes: that is the generation of dislocations and the formation of discrete slip bands on one or more of the six {110} slip planes operative at room temperature.

The following model, first proposed by Evans *et al* [8], considers the generation of dislocation loops from the edge of a cubical cavity. This is the simplest case, but the model could also be applied to spherical cavities and particles. The model proposed that, when the theoretical shear stress is reached at the interface, near a cavity corner, a rearrangement of atoms may occur so that an "extra (110) half-plane" emanating from a distorted (010) face and extending to the (1$\bar{1}$0) plane containing the cavity edge OZ is produced and in Fig. 8 ABCD is this "half-plane". By symmetry, on the other side of the cavity edge OZ, PQRS should be created and similarly for all twelve cavity edges. Therefore, the six pairs of primary {110} slip planes containing a cavity edge will each have two dislocations, for example BC and QR, of the same Burgers vector. These edge dislocations lie in a (1$\bar{1}$0) slip plane but the dislocation segments PQ, RS, AB and CD will be sessile at room temperature, lying

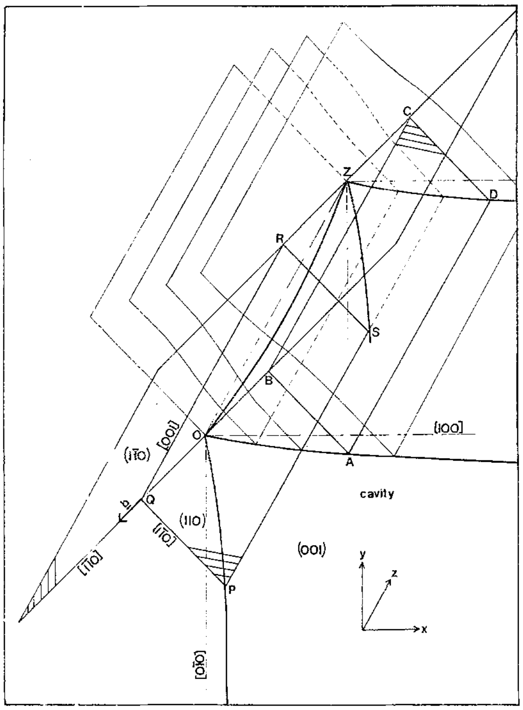

Figure 8 A model for pressurization-induced generation of dislocations on the (1$\bar{1}$0) slip plane containing the [001] edge of a cubical cavity. Note the "extra half-planes" ABCD and PQRS bounded by edge dislocations with $\boldsymbol{b} = \frac{1}{2}\, a$ [110] and $\frac{1}{2}\, a$ [$\bar{1}\bar{1}$0] which are glissile only in (1$\bar{1}$0), i.e. the segments BC and QR.

in (100) planes. BC and QR are potential Frank-Read sources, but in LiF, perhaps as a result of the stress gradient, appear not to act [9]. It is suggested, however, that the edge dislocations such as BC bow out and move along the slip plane away from the cavity edge retaining a half-loop configuration. It is proposed that further dislocations are created on the same or adjacent (1$\bar{1}$0) planes and the resultant glide of these dislocations is controlled by the local stress field.

A number of attempts have recently been made to identify the criterion for dislocation generation under superposed hydrostatic pressure [19-21]. Stress, strain and energy were considered and recent reviews [8, 9] clearly show that misfit strain is not the critical parameter in the majority of systems investigated, though it might be for small voids in LiF. The energy analysis of Ashby and Johnson [19] presupposes the existence of a glide loop which transforms to a prismatic loop; this situation certainly does not apply to the MgO matrix now studied in which any existing dislocations are immobile [17]. Therefore let us first examine stress criteria which supposes that at the matrix/discontinuity interface the matrix theoretical shear strength is reached locally.

Das and Radcliffe [20] and independently Ashby *et al* [21] have considered the stress around spherical cavities and inclusions in an isotropic matrix, subjected to hydrostatic pressure, P, and have evaluated the maximum shear stress, $\tau_{\max}$, which develops at the inclusion-matrix interface. For a spherical cavity with zero internal pressure $\tau_{\max} = 0.75\, P$ and for a spherical elastic inclusion:

$$\tau_{\max} = \frac{3G}{K}\left(\frac{K - K_i}{3K + 4G}\right) P \qquad (1)$$

where G is the shear modulus of the matrix and K and K_i are the bulk moduli of the matrix and inclusions, respectively.

Smart [22] has recently derived expressions for the shear stress around a cubical cavity in an isotropic solid subjected to hydrostatic pressure using a modified Muskhelishvili [23] and Savin [24] approach. She calculated values of $\tau_{\max}$ for two radii of curvature, r, of the corners. For r of $0.015a$ (where a is the perimeter of one face of the cavity) $\tau_{\max}$ is $3P$ and when the radius of curvature is taken to be $0.0061a$, $\tau_{\max}$ is $4.5P$.

Contrary to experimental observations none of all these calculations predict a size dependence. Experimentally, however, as other workers report for different systems [2, 8, 21], it was found that a large cavity produced dislocation arrays at a much lower pressure than a smaller cavity.

The values of the maximum shear stress at the interface between the matrix and the voids, at the minimum pressure at which dislocations were observed, evaluate to $7.7 \times 10^{-3}\, G$ and $4.0 \times 10^{-3}\, G$ for a cubical cavity (assuming Smart's approximations) for P of 0.2 GN m^{-2}, and $5.0 \times 10^{-3}\, G$ for a spherical cavity for P of 1 GN m^{-2}. All these values are small compared to the theoretical shear stress of the material, which would be of the order of $10^{-1}\, G$ [17], but are comparable to those evaluated by Evans *et al* [8, 9] for cubical and spherical cavities in LiF. For the case of precipitates, if they are assumed to be spherical and of Fe, Equation 1 predicts a very small $\tau_{\max}$ because the bulk moduli of MgO and Fe are not substantially different: 1.67×10^2 and 1.68×10^2 GN m^{-2}, respectively. It must be pointed out, however, as it has been previously by e.g. Das and Radcliffe [20] who observed dislocation generation in a W matrix at 3.3×10^{-3} G, that real interfaces will contain many stress raising irregularities, particularly precipitate/matrix interfaces. Dislocation generation has indeed been observed under a small indentor at a pressure of 10^{-3} G [25]. Thus it is not considered unreasonable that simple analyses underestimate the effects of localized stress raisers at interfaces.

Pressure and precipitate or void-size dependence of the generated dislocation density are, of course, quantitatively predicted by any strain criterion. The simplest, assuming isotropic continua, makes use of the Brookes' relation [26] for the critical misfit:

$$\frac{n\boldsymbol{b}}{r} = \frac{P}{3}\left[\frac{1}{K_{\mathrm{i}}} - \frac{1}{K}\right] \qquad (2)$$

where $\boldsymbol{b}$ is the Burgers vector, r the spherical inclusion radius and n the number of generated dislocations, is one. For Fe precipitates this analysis is, of course, again inadequate. For voids, however, P_{crit} evaluates to values well below the observed, e.g. 0.02 GN m^{-2} for r of 10 μm. Because of the order of magnitude difference, a strain criterion cannot be accepted. Therefore it is thought reasonable to conclude that *locally* the theoretical shear strength of the matrix is reached, at which point dislocation generation occurs. At this stage [27] mismatch strain should play a role in controlling the number (n of Equation 2) of dislocations created.

These calculations on cubical and spherical cavities produce in fact reasonable correlations between calculated and experimentally determined values of n. For a cubical cavity of edge 10 μm, for instance, following a 1 GN m^{-2} pressurization $\sim$ 50 dislocations are expected from each source on the cavity surface and experimental observations give this figure. For P of 2 GN m^{-2} calculation of the strain at interface of spherical cavity of radius 10 μm produced n of 100, whereas experimentally $\sim$ 50 were observed. This situation resembles those of the LiF/void [8] and Cr/Cr_2O_3 [27] systems, for which also it is generally considered that a stress criterion determines dislocation generation.

The mobility of the pressure-induced dislocations, at stresses above 0.5 yield stress, contrasts with the behaviour of relatively pure LiF [9] in which dislocations are immobile until $\sim$ 3% flow stress is reached. The marked lowering of the yield stress of a pressurized MgO crystal containing many Fe precipitates indicates that the pressure-induced dislocation arrays are suitable nuclei for the formation of multiple cross-glide throughout the crystals.

The micrographs of the dislocation arrays show that both conjugate (90°) and oblique (120°) intersections occur and that at high pressures cracks in $\{110\}$ are associated with slip band interactions. Kear *et al* [28] have discussed in detail the intersection of oblique slip systems and have suggested the following reaction:

$$\tfrac{1}{2}\, a\, [10\bar{1}] + \tfrac{1}{2}\, a\, [0\bar{1}1] = \tfrac{1}{2}\, a\, [1\bar{1}0] \qquad (3)$$

is the most likely result of the interaction. The resulting dislocation, $\boldsymbol{b} = \frac{1}{2}\, a\, [1\bar{1}0]$, is confined to move on the (112) plane and is thus sessile at room temperature. Keh *et al* [29] suggested that cracks are nucleated by piling up of dislocations against the sessile dislocations formed in this reaction. MgO deformed at ambient temperature has also been observed by Stokes *et al* [30] to contain cracks resulting from conjugate slip. Hence the production of cracks on $\{110\}$ planes is not surprising, since the shear in this region will be extremely anisotropic and heterogeneous due to the presence of intersecting slip bands and sessile dislocations. The presence of $\{100\}$ cracks can only be tentatively explained. It is thought that the material around the cavity cannot deform plastically any further and the additional strain is accommodated by simple cleavage on a $\{100\}$ plane.

We shall now consider the effect of the pressurization-induced dislocations on the mechanical properties of MgO in terms of the Johnston-Gilman theory [31]. Our results indicated that a decrease in the flow-stress of up to 10% occurs in single crystal MgO containing precipitates after pressurization. The density of precipitates was about 5×10^{7} cm^{-3} and the average length of dislocation line per precipitate is estimated to be 4 cm. The total pressurization-induced dislocation density is then 2×10^{8} cm^{-2}. If the dislocation velocity, v, is:

$$v = k\left[\frac{\sigma}{\sigma_0}\right]^{m} \qquad (3)$$

where k is 1 cm sec^{-1} and σ_0 and m are constants, the latter is estimated to be $\sim$ 50 from the strain rate dependence of the flow stress. Let us also assume that the mobile dislocation density in an unpressurized crystal, ρ_0, is 3×10^6 cm^{-2} (which is consistent with an absence of a yield drop) and that only a small fraction, say 10%, of the pressurization-induced dislocations, ρ_P, are mobile. Then, if $\rho_0 + \rho_P$ is 2.3×10^7 cm^{-2}, the drop in flow stress evaluates to 4%. Thus only a small decrease in the flow stress is expected ($<$ 10% was observed experimentally) despite the high density of pressurization-induced dislocations.

The existence and mobility of these pressurization-induced dislocations may not only affect flow but also fracture properties, especially if in a polycrystalline material mobile dislocations are present in all the grains. The results of the measurements of fracture stress and thermal shock resistance indicate, however, that the fracture stress of this particular material was unaffected by pressurization.

Pressurization of this material, however, did alter the critical temperature difference, ΔT_C, above which, on quenching, a catastrophic drop in fracture strength is observed. This is thought to be due to the inability of the material to accommodate thermal strains by elastic deformation which results in crack growth [32]. It is suggested that this growth was inhibited by the pressurization-induced mobile dislocations present, it is hoped, in each grain. These should be able to move within their grains under the thermal stresses and thus accommodate some of the thermal strain. The strain due to the movement of dislocations is, approximately, $\epsilon = nb\bar{x}$, where n is the length of dislocation line per unit volume, $\boldsymbol{b}$ is the Burgers vector and $\bar{x}$ is the mean distance moved by the dislocations. If the additional thermal strain ϵ_{th} due to an increase in ΔT_C of 55 K is 10^{-3} and this be equated to ϵ, $n\bar{x}$ evaluates to 3×10^{-4} cm^{-1}. If we now assume that, on average, dislocations move half a grain diameter, 15 μm, then n evaluates to $\sim 2 \times 10^7$ cm^{-2}. This figure compares favourably with 2.3×10^8 cm^{-2}, total, and 2.3×10^7 cm^{-2} mobile, density estimated previously for our MgO/Fe system and the results on the Cr/Cr_2O_3 system [14, 27] which indicate that realistic values for the total pressurization-induced dislocation densities are in the range 10^7 to 10^9 cm^{-2}. It is therefore suggested that the observed increase in ΔT_C is due to the movement, during quenching, of the pressurization-induced dislocations. These dislocations should, in principle also affect the fracture strength through an increase in the work of fracture term in a Griffith-type relation [33], which was not observed in our material.

Extension of this work to material of low porosity and fine grain size, where plastic deformation at the crack tip should be a more important factor, is therefore being carried out.

Acknowledgements

This work is part of a programme supported by the Science Research Council. The project on the thermal shock of MgO was supported by Chalmers University, Sweden, and the authors acknowledge Mr S. Persson and Dr Helgesson for their help and provision of specimens. The writers acknowledge also the provision of facilities by Professor D. Bijl and critical comments and discussion by Dr B. A. W. Redfern and Dr R. A. Evans.

References

1. F. P. BULLEN, F. HENDERSON, M. M. HUTCHINSON and H. L. WAIN, *Phil. Mag.* **9** (1964) 285.
2. A. BALL and F. P. BULLEN, *ibid* **22** (1970) 301.
3. T. E. DAVIDSON, J. C. UY and A. P. LEE, *Trans. Met. Soc. AIME* **233** (1965) 820.
4. B. A. W. REDFERN, R. A. EVANS and A. S. WRONSKI, *J. Mater. Sci.* **5** (1970) 789.
5. R. A. EVANS, B. A. W. REDFERN and A. S. WRONSKI, *Phil. Mag.* **23** (1971) 731.
6. A. S. WRONSKI, R. A. EVANS and B. A. W. REDFERN, "Solids Under Pressure" (edited by H. Ll. D. Pugh) (Inst. Mech. Eng., London, 1971) p. 94.
7. R. A. EVANS, B. A. W. REDFERN and A. S. WRONSKI, *J. Mater. Sci.* **7** (1972) 1216.
8. R. A. EVANS, A. S. WRONSKI and B. A. W. REDFERN, *Phil. Mag.* in press.
9. R. A. EVANS, Ph.D. Thesis, University of Bradford (1973).
10. P. W. BRIDGMAN, "The Physics of High Pressure" (Bell & Sons, London, 1949).
11. S. V. RADCLIFFE and H. WARLIMONT, *Phys. Stat. Sol.* **7** (1964) K 67.
12. A. BALL, F. P. BULLEN and H. L. WAIN, *Mat. Sci. Eng.* **3** (1969) 283.
13. F. P. BULLEN, F. HENDERSON, H. L. WAIN and M. S. PATERSON, *Phil. Mag.* **9** (1964) 803.
14. H. G. MELLOR and A. S. WRONSKI, *Acta Met.* **18** (1970) 765.
15. R. W. DAVIDGE, *J. Mater. Sci.* **2** (1967) 339.
16. S. A. BORTZ and H. H. LUND, "Mech. Props. of Eng. Ceramics" (edited by W. W. Driegel and H. Palmour) (Interscience, New York, 1961) p. 383.
17. R. J. STOKES, "Fracture" Vol. 7 (edited by H. Liebowitz) (Academic Press, New York, 1972) p. 157.
18. A. S. KEH, *J. Appl. Phys.* **31** (1960) 1538.
19. M. F. ASHBY and L. JOHNSTON, *Phil. Mag.* **20** (1969) 1009.

20. G. DAS and S. V. RADCLIFFE, *ibid* **20** (1969) 589.
21. M. F. ASHBY, S. H. GELLES and L. E. TANNER, *ibid* **19** (1969) 757.
22. N. SMART, private communication, see also [9].
23. N. I. MUSKHELISHVILI, "Some Basic Problems of the Mathematical Theory of Elasticity" (Noordhoff, Groningen, 1953).
24. G. N. SAVIN, "Stress Concentration around Holes" (Pergamon, Oxford, 1951).
25. J. FRIEDEL, "Electron Microscopy and Strength of Crystals" (edited by G. Thomas and J. Washburn) (Interscience, New York, 1963) p. 605.
26. H. BROOKES, "Metal Interfaces" (A.S.M., Cleveland, Ohio, 1962) p. 20.
27. A. S. WRONSKI, *Scripta Met.* **5** (1971) 851.
28. B. H. KEAR, A. TAYLOR and P. L. PRATT, *Phil. Mag.* **4** (1959) 665.
29. A. S. KEH, J. C. M. LI and Y. T. CHOU, *Acta Met.* **7** (1959) 694.
30. R. J. STOKES, T. L. JOHNSTON and C. H. LI, *Phil. Mag.* **4** (1959) 920.
31. W. G. JOHNSTON and J. J. GILMAN, *J. Appl. Phys.* **30** (1959) 129.
32. D. P. H. HASSELMAN, *J. Amer. Ceram. Soc.* **52** (1969) 600.
33. R. W. DAVIDGE and A. G. EVANS, *Mater. Sci. Eng.* **6** (1970) 281.

Received 27 November 1973 and accepted 11 January 1974.